VERSATILE CYCLIC P-Y CURVE FOR LATERAL PILE RESPONSE ANALYSIS

M. Hesham El Naggar, University of Western Ontario, London, Ontario, Canada
Nii Allotey, University of Western Ontario, London, Ontario, Canada

ABSTRACT
The beam-on-nonlinear-Winkler foundation (BNWF) model is widely used in the analysis of soil-pile-structure interaction due to its relative simplicity. Various BNWF models have been developed for different soils and pile-soil interface conditions. This paper highlights some important aspects of a versatile BNWF model recently developed by the authors, which can be used for cyclic lateral pile response in nonlinear time-domain soil-structure interaction (SSI) analyses. The specific features discussed include: the backbone curve; different loading, unloading and reloading rules; cyclic hardening/degradation of soil stiffness and strength; and gap formation with an option to allow for soil cave-in. Several example hysteretic loops are presented to illustrate the versatility of the model.

RÉSUMÉ
Le modèle de poutre-sur-la fondation de Winkler non linéaire (PFWN) est largement utilisé dans l'analyse de l'interaction sol-pieu-structure à cause de sa simplicité relative. Des divers modèles de PFWN ont été développés pour les différents sols et conditions d'interface de pieu-sol. Cet article présente quelques aspects importants d'un modèle adaptable de PFWN récemment développé par les auteurs, qui peut être utilisé pour le comportement latérale cyclique de pieu dans les domaines du temps non linéaire de l'analyse de l'interaction dynamique sol-structure (ISS). Les caractéristiques discutées incluent: courbe squelette; chargement différent, règle de déchargeant et rechargeant; le durcissement/adoucissement cyclique de rigidité et capacité de sol; et la formation d'écart avec une option pour tenir compte de l'effondrement de sol. Plusieurs exemples d'hystérèse sont présentés pour montrer l'adaptabilité du modèle.

1. INTRODUCTION

1.1 Soil-pile-structure interaction modeling

The response of structures supported on piles under imposed ground motion is directly linked to the responses of both the superstructure and substructure (foundation) through the process of soil-pile-structure interaction (SPSI). SPSI comprises two main components: kinematic interaction and inertial interaction. The substructure is first excited, which then transfers forces to the superstructure (kinematic interaction). The superstructure then transfers a subsequent feedback to the substructure (inertial interaction). In pile foundation systems, the inertial interaction component has been identified to significantly influence the response of the upper part of the pile foundation, while the kinematic interaction component has been identified to affect deeper portions of the pile foundation (Gazetas & Mylonakis 1999). Procedures used for dynamic pile response analysis range from soil discretization methods (i.e., finite difference, finite element and boundary element approaches) to soil spring model approaches. Using the former with adequate soil constitutive models, it is possible to solve the SSI problem as a whole, taking into account different loading and system response conditions. With advancements in computer speed, the time required for this type of analysis has decreased considerably. However, for systems involving extensive nonlinear behaviour, such analysis still requires a considerable amount of time. In addition to this, the approach remains unattractive to many design engineers, chiefly among them being structural engineers, because it requires considerable expertise and experience in the modeling of both structural and geotechnical aspects of the SSI problem (Poulos et al. 2002). It is worthy of note that geotechnical engineers prefer the soil discretization approach with the structure modeled as a linear stick model, while, structural engineers concentrate on the full 3-D modeling of the structure, and employ very simplified elastic springs to represent the soil. A gap therefore exists in expertise comfort and is partly responsible for the overly simplistic view held by a number of design engineers with regard to the effects of SSI on structural response.

The use of the BNWF approach to model pile foundations is popular among structural engineers. It has the ability to account for nonlinearity; and the load-transfer curves utilized to simulate the soil reactions can be evaluated easily from readily available empirical formulae. Some boundary element solution procedures are now even coupled with the BNWF approach to enable them account for soil nonlinearity (Kucukarslan & Banarjee 2003). Despite its popularity, many SSI experts are critical of the method because of its inability to model the soil as a continuum and its inherent assumption of decoupling the soil reactions at different elevations (i.e., ignoring shear deformations between different soil layers) and thus do not recommend it for the design of important projects. Notwithstanding, the BNWF approach is widely accepted in industry and has been shown to give satisfactory results for various laboratory and field experiments.

1.2 Existing BNWF models and programs

The BNWF approach has undergone considerable development since McClelland and Focht (1958) initially developed it for pile foundations. Figure 1 shows the normal force-displacement response curve obtained by Matlock in his laboratory experiment of a pile in Sabine River soft clay (Matlock 1970). Based on the experimental results, he established various curves relating the soil reaction, *p*, to the pile movement, *y*: namely, the static p-y curve, the cyclic p-y curve (pseudo-static) and the after cycling reload p-y curve.

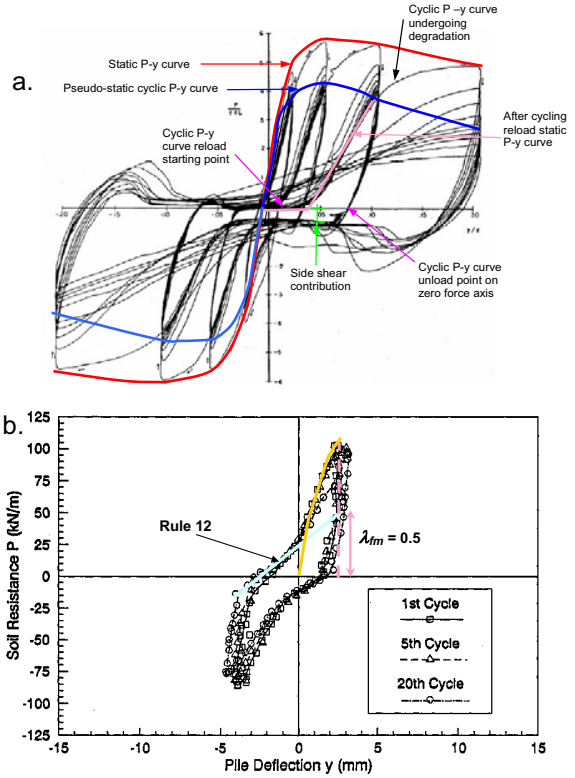

Figure 1. a) Normal force-displacement response of pile in Sabine River soft clay (after Matlock, 1970); b) cyclic P-y response at three pile diameters for pile in Ottawa sand of relative density 75% (after Dou and Byrne, 1996)

Many researchers followed this approach and there now exists a considerable data base of such curves for different soils. These curves can be used only for pseudo-static analysis and do not account for the cycle-by-cycle response depicted in Figure 1a. Commercial programs that are based on such formulations include COM624P (Wang & Reese 1993), LPILE (Ensoft 1997) and FLPIER (McVay et al. 1996). To account for nonlinearity in pile dynamics, the BNWF approach was extended by Matlock et al. (1978) to model the cycle-by-cycle response. They introduced an approach that utilizes the static p-y curve as a backbone curve and accounts approximately for cyclic degradation. Several variations of this approach have been implemented in available computer programs including: NONSPS (Kagawa 1983), PAR (PMB 1988), CYCPILE (Vazinkhoo et al. 1996b), PLYLAT (El Naggar & Bentley 2000), FLPIER(D) (Brown et al. 2001) and implementations in PEER's OpenSees (PEER 2000) computational platform (Boulanger et al. 1999). Each of these programs takes into account certain aspects of pile-soil behaviour evident in Figure 1 such as slack zone formation, cyclic degradation and side shear contribution. However, none of them seems to account efficiently for all the relevant aspects of the soil-pile response. Furthermore, most of these programs were developed from the geotechnical point of view with an emphasis on modeling of the soil medium but with poor modeling of nonlinear structural response features. On the other hand, some nonlinear structural analysis programs with nonlinear springs and gap elements have been used for SPSI (Wang et al. 1999). However, the ability of these programs to capture all the relevant soil response effects is limited. There is thus a need for focused efforts to address this issue. The work by Boulanger et al. (1999) represents an advancement in this direction, since their BNWF model was developed in the framework of the OpenSees platform, which features various structural and geotechnical modeling capabilities.

The model presented in this paper is part of an on-going research program at the University of Western Ontario aimed at developing SSI BNWF models in an existing nonlinear structural analysis program that can be used for the dynamic analysis of different SSI problems including shallow and deep foundations and retaining walls. The main objective of the work presented here is to develop a generic BNWF normal force-displacement response model capable of accounting for all the important aspects of the cyclic normal force-displacement response. The developed model is incorporated into a nonlinear structural analysis program (CANNY, Li 2002) that is currently used both in research and in industry for 3-D nonlinear static and dynamic analysis of structures. It has an extensive library of hysteresis models and allows for adding new ones.

2. DESCRIPTION OF MODEL

2.1 Backbone curve

The resistance of each soil layer to pile (or wall) movement is modeled using two compression-only spring elements on opposite sides of the pile. The static p-y curve defines the backbone curve and is based on an Iwan-like formulation using a multi-linear curve with four different segments. A schematic of the backbone curve is shown in Figure 2 (segments 1, 2, 3 and 4). The backbone curve can be either monotonically increasing (represented by solid lines in Figure 2), or can exhibit a post peak (residual) behaviour (segments 3 and 4 represented by dotted lines in Figure 2) to facilitate the modeling of stiff clays and dense sands. For monotonic backbone curves, the peak strength $p_f = p_3$, while for peak-post peak curves, $p_f = p_2$. The parameters needed

to establish the backbone curve (p_1-p_3, y_1-y_3, α_2, α_3) can be evaluated using graphical methods, or by curve-fitting algorithms such as that used by Joyner and Chen (1975). The multi-linear formulation renders the model more general and useful in capturing the main features of the response of different foundation systems and retaining walls under different loading conditions.

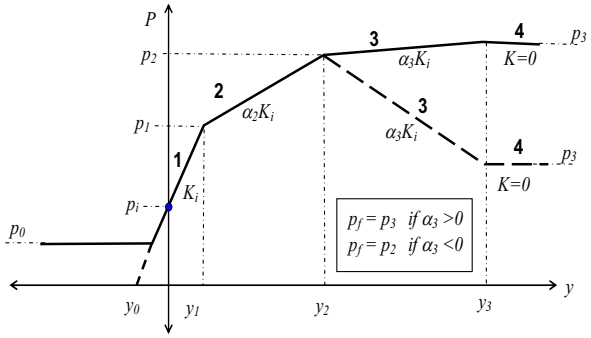

Figure 2. Model backbone curves

Figure 2 shows that the backbone curve can be shifted horizontally to the left allowing for an initial force (p_i) at zero displacement, and thus representing a pre-straining effect with displacement y_0, as would be the case for driven piles. It can also be shifted vertically (i.e., $p > 0$), which allows for modeling the soil reactions in the case of retaining walls, where the minimum force level, p_0, represents the active pressure experienced by the wall. Examples of such p-y response curves can be found in Briaud and Kim (1998) and Carubba and Colonna (2000).

2.2 Standard reload curve

Figure 3 shows an example of the unloading and reloading response curves. The reloading response which is termed the standard reload curve (SRC) (segments 7-8-9-10) follows the shape of the backbone curve (similar to Iwan formulation) but is scaled using the current force at the reload beginning point (p_{r0}, y_{r0}) based on Pyke's approach (Pyke 1979) with a slight modification (Eq. 1b). In Pyke's original model, strength degradation/hardening under cyclic loading was not accounted for, and the strength was assumed to be constant. In the present approach, since degradation/hardening is modeled, the scaling factor is calculated using the current strength, $\delta_t\, p_f$, where δ_t is the strength degradation/hardening parameter. A similar approach has been used by Lee (1993) for the analysis of the cyclic axial response of piles. For peak-post peak response, the SRC comprises segments 7-8-9, i.e, segments 9 and 10 merge together. The stiffness and strength degradation/hardening parameters, δ_k and δ_t are calculated based on the number of equivalent cycles (NEC) and are used to degrade or harden the backbone response at the beginning point of reloading. The equations of the various turning points of the SRC ((p_{r1}, y_{r1}) – (p_{r3}, y_{r3})) are shown in Figure 3. For the case where the SRC crosses the initial backbone curve, there are two options: either to follow the original backbone curve, similar to the extended Masing rule (Vucetic 1992); or to continue along the SRC. Unloading from the standard reload curve follows the general unloading response as discussed below.

$$\kappa = 1 + \frac{p_{u0}}{\delta_t\, p_f} \text{ - unloading} \qquad \kappa = 1 - \frac{p_{r0}}{\delta_t\, p_f} \text{ - reloading} \qquad \text{[1a,b]}$$

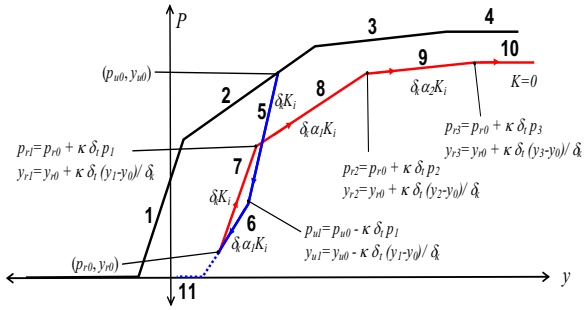

Figure 3. General unload and standard reload curves

2.3 General unloading curve

The general unloading curve (GUC) (segments 5-6) also follows a path similar to the shape of the backbone curve and is scaled using the modified Pyke approach based on the force at the beginning point of current unloading (p_{u0}, y_{u0}). Degradation/hardening behaviour is accounted for by modifying the backbone curve using the stiffness degradation/hardening parameter. Unloading occurs only in the first quadrant and the effect of strength degradation/hardening in this quadrant is not significant. Therefore, the model accounts for only stiffness degradation/hardening (i.e., δ_t = 1). The stiffness degradation parameter can be calculated based on the NEC, or can be set to a specific constant value. The equation for the turning point of the GUC (p_{u1}, y_{u1}) is also shown in Figure 3. The unloading phase entails a decrease in the soil reaction, p, until it reaches the minimum force level, p_0 (p_0 = 0 in Figure 3). For cases where reloading occurs before reaching the minimum force level, reload occurs along the SRC.

2.4 Movement at minimum force level and drag shear

When the soil resistance during the unloading phase reaches the minimum force level and the pile movement, y, continues in the negative direction, the soil resistance remains equal to the minimum force level (i.e., with zero stiffness). Two responses are possible along this segment of the unloading phase: the p = 0 case; and the $p > 0$ case. The p = 0 case models the condition where the pile/wall separates from the soil; and the $p > 0$ case models the case where the wall experiences a constant minimum soil reaction force (active force) as it moves away from the wall (as shown in Figure 2). For the p = 0 case, there exists an option to account for side shear force that could develop on

the sides of a pile as it moves through the slack zone (shown in Figure 1a).

It should be noted that the soil reactions are modelled using two compression-only springs, one on each side, as shown in Figure 4a. During the unloading phase, as the pile moves rightwards in the slack zone, the right spring accounts for the soil resistance, and the left spring provides no resistance, and vice versa. The left and right springs therefore contribute collectively to the response of the pile for movement in either the left or right directions.

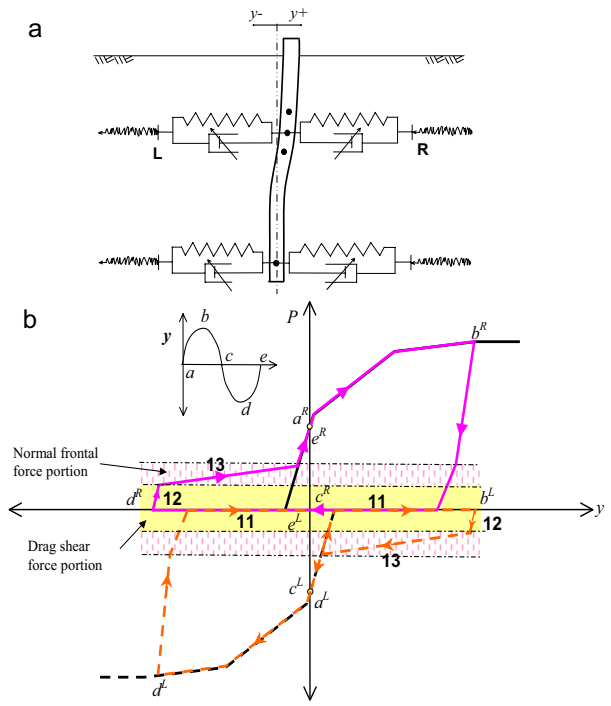

Figure 4. a) BNWF pile-soil system, b) typical responses of right and left springs

2.5 Direct reload curve (DRC)

The direct reload curve models the resistance of the soil in the slack zone and comprises two sections: the side shear component (segment 12) with a limiting force estimated as $\lambda_{sm}p_m$; and the normal frontal component with a limiting force of $\lambda_{fm}p_m$ (Figure 4b). λ_{sm} and λ_{fm} are the side shear force and normal frontal force factors, and p_m is the past maximum force experienced by the soil. The side shear component exists only for the case of $p = 0$.

When the pile separates from the soil over a sufficient depth, a portion of the unsupported soil caves-in and fills the gap. The soil that fills the gap exists in a loose state. As the pile moves back towards the soil that filled the gap, the soil gets re-compressed resulting in a strain-hardening type of response. This behaviour is observed in the form of S-shaped curves that characterize many experimental cyclic p-y loops (Figure 1b). S-shaped loops have been observed in pile tests in wet drained sand, liquefied sand and soft clays by many researchers. For soils such as over-consolidated clays that can stand unsupported, pure gaps form and the pile traverses the full gap distance before bearing on the soil again.

Figure 5 shows that the direct reload curve starts at the beginning of segment 12 and ends at the point Q that represents the intersection of the current SRC with its origin at point (0, y_{rl}), and segment 13 of the DRC. Subsequent loading past this point leads to movement along the SRC. Such an observation can be made from experimental results of cyclic p-y loops for pile tests in sands and clays (e.g.; Meymand 1998; Dou and Byrne 1992), and is linked to soil memory behaviour. Two standard reload curves are shown in Figure 5. Curve A represents the SRC corresponding to the case where a stable gap is formed. For this case, the pile travels all the way back to meet the soil where it separated, and reload occurs along this curve; the direct reload curve is thus a horizontal line on the zero force axis. This is the approach used in many BNWF programs to account for gap formation (e.g., FLPIER (D) and PYLAT). Curve B shows the same curve shifted to the left by an amount Δy_s. This distance is linked to the amount of soil cave-in and can be explained as follows. The strain-hardening behaviour is associated with a decrease in the voids ratio and an increase in the mean effective confining pressure, which can be modeled by two springs in series: an inner spring representing the loose soil and an outer one representing the original soil (Insert X in Figure 5). As the soil compresses, the combined stiffness of the two springs is controlled by the loose soil, which experiences most of the deformation and densifies.

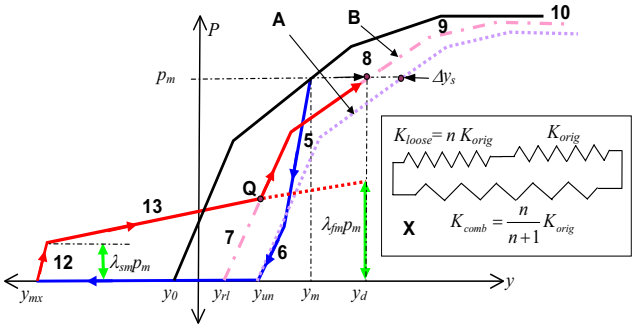

Figure 5. Direct reload curve with insert (X) showing schematic of spring representation of loose and original soil

The stiffness of the loose soil increases as its density increases, and thus contributes more to the overall stiffness of the two-spring system. This process continues until the stiffness of the loose soil reaches the value of the stiffness of the original soil. The strain-hardening curve should thus intersect with curve A; however, this is not the case and it rather intersects with curve B. This is due to the compressed loose soil under a mean effective pressure similar to that existing in the original soil occupying a finite volume of the gap formed. This infers that more soil cave-in

results in larger shifts of the curve B as Gohl (1992) and Barton (1982) have shown for pile tests in sand. Both researchers observed that under two-way cycling action the pile always experiences a residual displacement in the direction of the initial motion as a result of a larger amount of soil fall-in at the beginning of the cycling action, due the surrounding soil being less dense at the beginning of shaking.

Typical values of the parameters that define the DRC can be estimated from experimental results of cyclic p-y curves. For a pure gap condition λ_{sm} = 0 and λ_{fm} = 0. For confined p-y responses (e.g. at the lower portion of piles in dry loose sand) significant cave-in occurs and λ_{fm} = 1. The values of λ_{sm} and λ_{fm} evaluated from Figure 1b are 0 and 0.5, respectively, for piles in drained sand of relative density 75% (Dou & Byrne 1996).

The origin of curve B at the minimum force level (0, y_{rl}) has been estimated empirically by the authors using results from a large number of one-way, two-way and intermediate constant cyclic field load tests of piles in sand compiled by Long and Vanneste (1994). The resulting curve from these tests is shown in Figure 6 and indicates the effect of type of loading, which is directly linked to the effect of soil cave-in on the cyclic response. In Figure 6, ϕ_h is the ratio of the maximum distance moved at the minimum force level, to that for the case of a constant force two-way cyclic loading and varies from -1 to 0. The case ϕ_h = -1 represents two-way cyclic loading, and ϕ_h = 0 represents one-way cyclic loading where no soil cave-in is possible and β_h = 1. For two-way cyclic loading, the maximum amount of soil cave-in is possible, and β_h corresponds to the value of β_h at ϕ_h = -1. In between these extremes, the hyperbolic curve shown in the figure models the expected effect of soil cave-in. A value of Λ = 5 fit the proposed values given by Long and Vanneste (1994); however, these were mean value estimates, and the value of β_h at ϕ_h = -1 ranges approximately between 0.1 – 0.3.

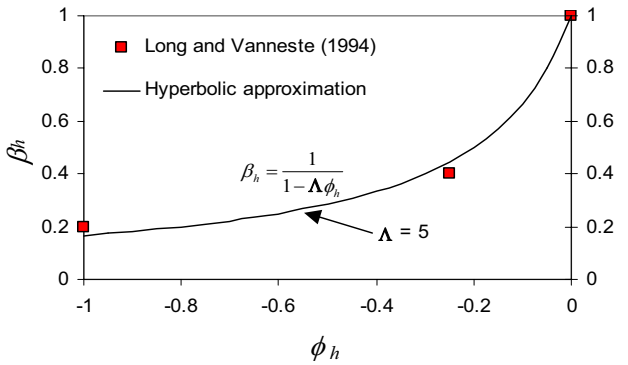

Figure 6. Empirical curve for estimating the point of origin of the current SRC

Based on this formulation, the expressions for the various parameters are shown in Eq. 2.

$$y_{rl} = y_0 + \beta_h \left(y_{un} - y_0 \right) \qquad \beta_h = \frac{1}{1 - \Lambda \phi_h}$$

$$\phi_h = \frac{y_{mx} - y_{un}}{y_m + y_{un} - y_0} \qquad \text{[2a,b,c]}$$

In these equations, y_{mx} is the maximum displacement at the minimum force level, y_m is the displacement corresponding to a two-way cyclic action and y_{un} is the displacement at the start of movement at the minimum force level. For the case of no soil cave-in β_h = 0.

2.6 Estimation of degradation/hardening parameters

Degradation/hardening of the backbone curve is estimated using an equivalent number of cycles approach using the S-N response curve as known in fatigue studies, or the soil cyclic strength curve as known in soil dynamics, as a weighting function. This curve defines the number of loading cycles necessary to initiate or attain a specified soil response condition. This could be the attainment of a unit pore pressure ratio as used in liquefaction initiation prediction, the development of a specified amount of cyclic or residual strain (e.g., 5% double-amplitude cyclic strain, 10% residual strain), or the development of a specified amount of volumetric soil strain resulting from cyclic soil compression of cohesionless soils. The S-N response curve, shown in Figure 7, can be developed from cyclic triaxial or simple shear testing and is readily available in the literature for different types of soil. Most BNWF models account for cyclic degradation/hardening using soil specific empirical formulations derived either for only uniform one or two-way cyclic loading. Using the S-N curve makes it possible to model non-uniform irregular loading conditions. The S-N curve is characterized by the N=1 intercept, S_{N1},

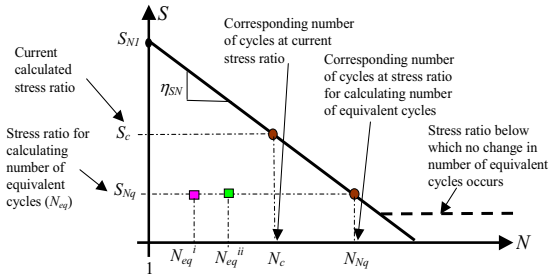

and the slope of the line, η_{SN}. Either a log-log model or semi-log model can be chosen to represent the S-N curve.

Figure 7. Schematic of S-N curve

$$N_{eq}^{ii} = N_{eq}^{i} + 0.25 \frac{N_{Nq}}{N_c} \qquad \text{[3]}$$

A modified NEC (Seed et al. 1985) approach is used to evaluate the NEC. The NEC is calculated based on Eq. 3 at each unload or reload (quarter of a cycle – represented by 0.25 in Eq. 3). In this approach, the stress ratio at which the NEC is calculated is not fixed at $0.65S_{mf}$, but at a user-specified input (S_{Nq}). S_{mf} is the maximum force/stress ratio experienced by the system over the entire loading history. The maximum force/stress ratio is not known prior to performing the analysis, however, theoretically, it does not affect the computed NEC (Annaki and Lee, 1977). This was confirmed through a parametric study conducted by the authors for the range of S_{Nq} between 0.3 – $0.85S_{mf}$. Other researchers (e.g. Lee and Chan 1972) have used values between 0.65 - $0.85S_{mf}$.

After calculating the NEC, the stiffness and strength degradation/hardening factors δ_k and δ_t are estimated using the elliptical equations given in Eq. 4, where the subscript *k* refers to stiffness and *t* to strength.

$$\delta_{k,t} = \begin{cases} 1 & N_{eq} < 1 \\ 1 + \left(\delta_{km,tm} - 1\right)\left[1 - \left(\dfrac{N_{Nq} + 1 - N_{eq}}{N_{Nq}}\right)^{\theta_{k,t}}\right]^{1/\theta_{k,t}} & 1 \le N_{eq} \le N_{Nq} + 1 \\ \delta_{km,tm} & N_{eq} > N_{Nq} + 1 \end{cases} \quad [4]$$

These elliptical equations can model various forms of degradation/hardening events. If $\delta_{km,\,tm}$ is less than one, the equation models a degradation event; if it is greater than one, it models a hardening event. For both cases, the value of the parameter $\theta_{k,\,t}$ determines whether the curve is concave or convex (i.e., whether it bulges away from or towards the horizontal axis). It should be noted that in the literature, degradation is modeled only with convex curves while hardening is modeled with concave curves.

2.7 Modeling of radiation damping

Radiation damping is modeled using a damper placed in parallel with each spring element. Recent work by Wang et al. (1999) has shown that placing a linear damper in parallel with a nonlinear soil spring as implemented in SPASM8, PAR, etc., can result in unrealistically large damping forces. This is due to forces bypassing the hysteretic system by way of the parallel linear dashpot. This is the case especially for soft soils under strong shaking conditions where considerable soil nonlinear behaviour occurs. Nonetheless, for cases where soil-pile relative displacements only slightly exceed the elastic range, parallel linear dashpot radiation damping gives reliable results. In general, Wang et al. (1999) found that series-radiation damping is more realistic than parallel-radiation damping, and agreed well with the damping of the inner and outer fields of the dynamic BNWF implementation by Nogami et al. (1992). This approach models the physical behaviour of scattered waves, since they originate from the inner field and are dispersed/dissipated in the outer field. Badoni and Makris (1996) limited the value of the damping force that could be developed in their parallel damper implementation of a BNWF model, by relating the limiting damping force to the yield displacement. This approach is in line with work by El Naggar and Bentley (2000) who implemented a nonlinear spring to represent the near field in series with a linear damper and a linear spring to represent the far field, and showed that this combination could be simplified into a nonlinear spring in parallel with a nonlinear damper. This approach is implemented in the current model.

Eq. 5 gives the equations governing the model, which represents a stiffness proportional damping model. This means the damping factor is directly related to the current soil stiffness. The initial value of the damping constant is evaluated from the elastic impedance functions proposed by Novak et al (1978) and given in Eq. 5b. In Eq. 5, a_o is the dimensionless frequency; G_{max} and ν are the small-strain shear modulus and Poisson ratio, respectively; *c* is the damping constant; *K* is the current soil stiffness and P_d and $\dot{u}$ are the damping force and relative velocity, respectively.

$$P_d = \left[c(a_o)K\right]\dot{u} \qquad c(a_o) = G_{\max} S_u(a_o, \nu) \qquad [5a,b]$$

Based on this model, as the stiffness changes the damping force also changes, which is in accordance with the approach by Badoni and Makris (1996). An interesting aspect of the model is that when movement occurs in the slack zone, the computed radiation damping is small, and as would be expected, becomes entirely zero for the case of a pure gap. Also, degrading system responses result in a reduction in radiation damping, while, hardening system responses result in an increase in radiation damping, which is also to be expected.

3. TYPICAL MODEL RESPONSES

The developed model can be used to model different soil-pile systems under various loading conditions. This includes uniform load or displacement controlled loading regimes commonly used in field and laboratory tests. Typical example hysteretic loops for load-controlled tests are presented in this section to highlight the different capabilities of the model. These loops are obtained for a soil with S-N curve parameters S_{N1} = 0.8, η_{SN} = -0.1 with S_{Nq} taken as 0.5, under an initial confining pressure of 100 kPa. The various backbone curves are obtained from typical p-y curves for different soils.

3.1 One-way loading examples

Figures 8a and b represent the response of the spring in the direction of the load under a one-way cyclic loading action. Figure 8a shows a degrading response, while Figure 8b shows a hardening response. In Figure 8a only stiffness degradation has been accounted for. This represents the response of undrained soft clays, which generally undergo stiffness degradation under cyclic action, but not much strength degradation. In Figure 8b, both stiffness and strength hardening are accounted for representing the response for dry sandy soils. The response of the system for different values of the elliptical degradation/hardening

parameter (θ_k, θ_t) is shown in both figures. In Figure 8a, it takes 7, 8 and 9 cycles to achieve a maximum displacement ratio of about 16 for θ_k = 0.5, 1.0 and 2.0, respectively. The minimum degradation amount (δ_{km}) is achieved at these points and further increase in the number of cycles, results in similar increases in the displacement ratio for the different cases. This is evident from the last two loops. In Figure 8b, a maximum displacement ratio of 15, 12 and 9 can be observed under 8 cycles of loading for $\theta_{k,t}$ = 0.5, 1.0 and 2.0, respectively. These figures show that for the case of hardening, the response for higher initial hardening rates results in smaller permanent displacements, while for degradation, higher initial degradation rates result in larger permanent displacements.

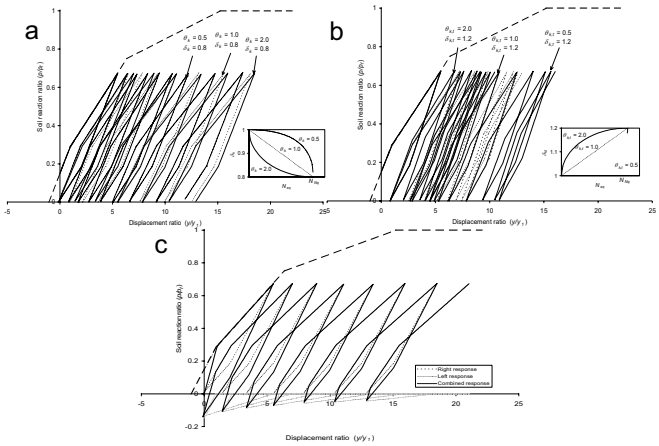

Figure 8: Typical response of single spring under one-way loading undergoing a) degradation; b) hardening; and c) response of combined spring under one-way loading

In Figures 8a and 8b, only the response of the spring in the direction of the load is shown, since this mainly controls the response under one-way loading. Figure 8c shows the combined response for both springs. For the case when an initial confining pressure exists as is shown in the figure, both left and right springs contribute to the initial stiffness, and the stiffness of the combined response is twice that of each. Also, for the case of soil cave-in, or when a side shear contribution exists, unload passes the zero force axis and enters the negative region. Examples of similar one-way p-y loops for pile tests in sand that exhibit this feature can be found in Vazinkhoo et al (1996a).

3.2 Two-way loading examples

Figures 9a and b show typical two-way cyclic p-y loops for both a degrading unconfined response and a hardening confined response. The degradation/hardening parameters are the same as those used in Figure 8, with Λ = 5, λ_{sm} = 0.02, and λ_{fm} = 0.5 and λ_{fm} = 1.0 in Figures 9a and 9b, respectively. From the figures, the S-shape and elliptical shape typical of unconfined and confined responses can be observed. In the case of Figure 9a, the degrading response results in an increase in displacement, while in Figure 9b the hardening response results in a slight reduction in displacement. Both types of responses are commonly observed from field and laboratory experiments.

Figure 9c also shows a typical varying-load two-way cyclic loading response with peak-post peak behaviour. The peak-post peak behaviour is typical of mainly overconsolidated stiff clays. In this case a pure gapping mechanism is modeled. Reload of a given side therefore only occurs after the pile traverses the full gap distance. Λ = 0, λ_{sm} = 0 and λ_{fm} = 0.

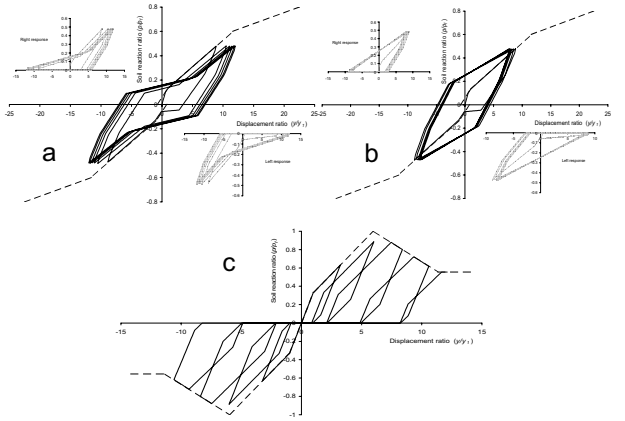

Figure 9: Typical two-way a) unconfined response with degradation; b) confined response with hardening; and c) peak–post peak response with pure gap formation

4. CONCLUSIONS

A BNWF normal force-displacement model has been developed for SPSI that accounts for various aspects of the SPSI response. The different aspects of the model discussed include the type of the backbone curves, the unloading and reloading response curves, the modeling of soil cave-in, and the modeling of degradation/hardening. Various example p-y loops under one-way and two-way loading were then presented.

5. REFERENCES

Annaki, M., Lee, K.L.L. 1977. Equivalent uniform cycle concept for soil dynamics. Journal of Geotechnical Engineering Division, ASCE, Vol. 103, GT6, pp. 549-564

Badoni, D., Makris, N. 1996. Nonlinear response of single piles under lateral inertial and seismic loads, Soil Dynamics and Earthquake Engineering, Vol. 15, pp. 29-43.

Barton, Y.O. 1982. Laterally loaded model piles in sand: centrifuge tests and finite element analysis, PhD Thesis, Cambridge University, UK.

Boulanger, R.W., Curras, J.C., Kutter, B.L., Wilson, D.W., Abghari, A. 1999. Seismic soil-pile-structure interaction experiments and analysis, Journal of Geotechnical and Geoenvironmental Engineering, ASCE, Vol. 125, No. 9, pp. 750-759.

Briaud, J.L., Kim, N.K. 1998. Beam-column method for tieback walls, Journal of Geotechnical and Geoenvironmental Engineering, ASCE, Vol. 124, No. 1, 67-79.

Brown, D.A., O'Neill, M.W., Hoit, M., McVay, M., El Naggar, M.H., and Chakrabotry, S. 2001. Static and dynamic lateral loading of pile groups, NCHRP Report 461, Transportation Research Board, Washington, D. C.

Carubba, P., Colonna, P. 2000. A comparison of numerical methods for tied walls, Computers and Geotechnics, Vol. 27, pp. 117-140.

Dou, H., Byrne, P.M. 1996. Dynamic response of single piles and soil-pile interaction, Canadian Geotechnical Journal, Vol. 33, pp. 80-96.

Gohl, W.B. 1990. Response of pile foundation to simulated earthquake loading: experimental and analytical results, PhD Thesis, University of British Colombia, Vancouver, B. C.

El Naggar, M.H. and Bentley, K.J. 2000. Dynamic analysis for laterally loaded piles dynamic p-y curves, Canadian Geotechnical Journal, Vol. 37, pp. 1166-1183.

Ensoft 1997. LPILE for Windows, Technical and User's Manual, Austin, Texas.

Gazetas, G., Mylonakis, G. 1998. Seismic soil-structure interaction: new evidence and emerging issues, Geotechnical Earthquake Engineering and Soil Dynamics-III, ASCE Geotechnical Special Publication No. 75, eds. P. Dakoulas, M. Yegian, & R.D. Holtz, pp. 1119-1174.

Joyner, W.B., Chen, A.T.F. 1975. Calculation of nonlinear ground response in earthquakes, Bulletin of the Seismological Society of America, Vol. 65, No. 5, pp. 1315-1336.

Kagawa, T. 1983. NONSPS: User's Manual, McClleland Engineers Inc., Houston, Texas.

Kucukarslan, S. and Banarjee, P.K. 2003. Behaviour of axially loaded pile group under lateral cyclic loading, Engineering Structures, Vol. 25, pp. 303-311.

Lee, C.Y. 1993. Cyclic response of axially loaded pile groups, Journal of Geotechnical Engineering, ASCE, Vol. 119, No. 9, pp. 1399-1413

Lee, K.L.L., Chan, K. 1972. Number of equivalent significant cycles in strong motion earthquakes, Proc. International Conf. on Micro-zonation, Vol. II, Seattle, Washington, pp. 609-627.

Li, K. 2002. CANNY Version. C02, Technical and User's Manual, CANNY Structural Analysis, Vancouver, B.C.

Long, J.H. Vanneste, G. 1994. "Effects of cyclic lateral loads on piles in sands", Journal of Geotechnical Engineering, ASCE, Vol. 120, No. 1, pp. 225-243.

Matlock, H. 1970. Correlations for design of laterally loaded piles in soft clay, Proc. 2nd Offshore Technology Conf., Paper No. OTC 1204, Houston, Texas.

Matlock, H., Foo, S., Bryant, L. M. 1978. Simulation of lateral pile behavior under earthquake motion, Proc. ASCE Specialty Conf. on Earthquake Engineering and Soil Dynamics, Vol. II, Pasadena, California, pp. 600-619.

Meymand, P.J. 1998. Shaking table scale model tests of nonlinear soil-pile-superstructure interaction in soft clay, PhD Thesis, University of California, Berkeley.

McVay, M.C., Hays, C., and Hoit, M. 1996. Development of a coupled bridge superstructure–foundation finite element code. Final Report B-8415 for Florida DOT, University of Florida, Gainesville, FL.

Novak, M., Nogami, T., Aboul-Ella, F. 1978. Dynamic soil reactions for plane strain case. Journal of Engineering Mechanics Division, ASCE, Vol. 104, No. 4 pp. 953-959.

Nogami,T., Konagi, K., Chen, H. 1992. Nonlinear soil-pile interaction model for dynamic lateral motion, Journal of Geotechnical Engineering, ASCE, Vol. 118, No. 1, pp. 89-106.

PEER 2000. The Open System for Earthquake Engineering Simulation (OpenSees), http://opensees.berkeley.edu/

PMB Systems Engineering 1979. SPSS Phase 2, Final Report to Shell Oil Company.

Poulos, H.G., Carter, J.P., and Small, J.C. 2002. Foundations and earth retaining structures - research and practice, Proc. 15th Int. Conf. on Soil Mechanics and Geotechnical Engineering Istanbul, Turkey, Vol. 4, pp 2527-2606.

Pyke, R. 1979. Nonlinear soil models for irregular cyclic loadings, Journal of Geotechnical Engineering, ASCE, Vol. 105, No. GT6, pp. 715-726.

Seed, H.B., Idriss, I.M., Makdisi, F., Banerjee, N. 1975. Representation of irregular stress time-histories by equivalent uniform stress series in liquefaction analysis, Report No. UCB/EERC 75-29, University of California, Berkeley.

Vazinkhoo, S., Byrne, P.M., Lee, M.K. 1996a. A cyclic p-y curve model, Proc. 49th Canadian Geotechnical Conf., St. John's, Newfoundland, pp. 239-249.

Vazinkhoo, S., Byrne, P.M., Lee, M.K., and Foschi, R.O. 1996b. CYCPILE – A computer program for analysis of cyclic and monotonic lateral loads on single piles, Proc. 49th Canadian Geotechnical Conf., St. John's, Newfoundland, pp. 393-400.

Vucetic, M. 1990. Normalized behavior of clay under irregular loading, Canadian Geotechnical Journal, Vol. 27, pp. 29-46.

Wang, S.T., and Reese, L.C. 1993. COM624P — laterally loaded pile analysis program for microcomputer, version 2.0. Report FHWA-SA-91-048, Washington, D.C.

Wang, S., Kutter, B.L., Chacko, J.M., Wilson, D.W., Boulanger, R.W., and Abghari, A. 1998. Nonlinear seismic soil-pile-structure interaction, Earthquake Spectra, Vol. 14, No. 2, pp. 377-396.